

**APPLICATION OF THE TRANSIENT ELECTROMAGNETIC METHOD
(TEM) WITH LINKAGE OF WELL INFORMATION TO THE
GEOELECTRIC IMAGING OF THE RESENDE BASIN, BRAZIL**

*APLICAÇÃO DO MÉTODO TRANSIENTE ELETROMAGNÉTICO (TEM) COM VÍNCULO DE
INFORMAÇÕES DE POÇOS PARA O IMAGEAMENTO GEOELÉTRICO DA BACIA DE
RESENDE, BRASIL*

**Hans Schmidt SANTOS¹, Felipe Barbosa Venâncio de FREITAS², Jonas Jackson Lobão
RIOS¹, Nicolas Aguiar ACCIAINOLI¹, Nayara Pavan RODRIGUES¹**

¹Departamento de Pesquisa e Extensão, Faculdade Salesiana Maria Auxiliadora, Rua Monte Elísio, Distrito Visconde de Araújo,
Macaé – RJ. Brasil. E-mail: hans.schmidt@live.com.

²Programa de Mestrado em Geofísica, Observatório Nacional, Rua General José Cristino 77, Rio de Janeiro – RJ. Brasil.
E-mail: felipebvenancio@gmail.com

Introduction
Transient Electromagnetic Method - (TEM)
Description of the Resende Basin
Location
Available models
Electrical resistivity model
Gravimetric modeling of the Resende Basin
Process and results
Conclusions
References

ABSTRACT - This paper presents an improvement to the subsoil resistivity model of the Resende Basin, Brazil. In addition to 88 transient electromagnetic surveys, 39 wells distributed in the region were used. Through the acquired data, improvements were made to the resistivity model utilizing the known sediment depths of the wells as a link to estimate where the subsoil is more electrically conductive ($\rho < 300 \Omega.m$). Therefore, this study allowed the construction of a more realistic model of the subsoil conductivity, which allows the updating of previous geoelectric surveys and contribute to the knowledge of the subsoil of an important region in the hydrogeological context of Brazil.

Keywords: Subsoil Resistivity, Resende Basin, Transient Eletromagnetic Method.

RESUMO - Este trabalho apresenta uma atualização do modelo de resistividade do subsolo da Bacia de Resende, Brasil. Em adição a 88 sondagens transiente eletromagnéticas, dados de 39 poços distribuídos na região foram utilizados. Através dos dados adquiridos, melhorias foram feitas para o modelo de resistividade utilizando as profundidades de sedimentos conhecidas dos poços como vínculo para estimativa das regiões onde o subsolo é mais condutivo ($\rho < 300 \Omega.m$). Assim, esse estudo permitiu a construção de um modelo de condutividade do subsolo mais realista, o que permite atualizar pesquisas geoeletricas anteriores e contribuir para o conhecimento do subsolo de uma importante região no contexto hidrogeológico do Brasil.

Palavras-chave: Resistividade do subsolo, Bacia de Resende, Método Transiente Eletromagnético.

INTRODUCTION

The subsoil resistivity mapping has been used in various applications such as mineral exploration, hydrogeophysical studies, environmental studies and applications in geology and civil engineering. Methods based on electrical resistivity are important tools used in underground water research due to its ability to map low resistivity zones that may be associated with sediments or groundwater (Sorensen et al., 2000).

According to Santos (2005), the electric current propagation mechanisms in a material are related to the conductivity type which may be "electrolyte conductivity" that depends on the nature of the ions and concentration, in addition

to water flow in the rock pores and fissures; and "electronic conductivity" that depends on the presence of conductors such as metallic minerals or graphite in the rock formation.

The magnetic permeability and the dielectric constant can determine the electromagnetic properties of the subsoil and rocks. The resistivity method consists in generating artificial electric currents that are introduced into the subsoil where potential differences are obtained on the surface.

The deviations of the potential differences expected on soil provide various data about electrical properties and the subsurface inhomogeneities (Kearey et al., 2002).

The electromagnetic method instrumentation can take different forms. Most systems consist of a source that transmit a time-varying electromagnetic field.

Then, a receiver can measure the components of the total (primary and secondary) magnetic field, and an electronic circuitry can process, store and display the signals and the subsoil resistivity estimation (Delleur, 2006).

The Resende Basin is located in the southwest of Rio de Janeiro State, comprising an area of approximately 44,000 km². The basin has a great

geological and hydrographic heritage.

For this reason, the region was contemplated for resistivity studies through the transient electromagnetic method (Bettini, 2004).

Data of 88 transient electromagnetic soundings of the Resende Basin granted by the Observatório Nacional (ON) and data from 39 wells distributed throughout the basin were used.

The processing of the TEM soundings calibrated with well data was used to improve the resistivity mapping and contribute to the mineral underground water research.

TRANSIENT ELECTROMAGNETIC METHOD - (TEM)

According to Kearey et al. (2002), the material resistivity is defined through the electrical resistance between the opposing faces of an unit cube of the material. For a conductor cylinder with δR resistance, δL length and δA cross sectional area, the ρ resistivity is given:

$$\rho = \frac{\delta R \delta A}{\delta L} \quad (1)$$

The resistivity unit is $\Omega \cdot m$; the inverse of resistivity is called conductivity. When it is divided by 1000, the measured stays in miliSiemens (mS) per meter; mS/m (Delleur, 2006).

According to Peng & Zhang (2007), most physical property of rocks (such as mechanical and acoustic properties; hydraulic, thermal, and electrical conductivities) are determined to some extent on the fractures and the fluids contained. The porosity is the main control of the rock resistivity. The resistivity generally increases with porosity decreasing.

However, even the crystalline rocks with

insignificant intergranular porosity are conductive along fractures and fissures (Schmucker & Weidelt, 1975).

Figure 1 shows the expected resistivity range of the common types of rocks. Nevertheless, the effective resistivity is expressed in terms of the resistivity and the water volume present in the rock pores (Kearey et al., 2002).

The transient electromagnetic method (TEM) is an electromagnetic method that works with an artificial source operating in the time domain. The surveys are performed through a transmitter and a receiver as shown in Figure 2 (Santos, 2006).

The transient electromagnetic method is based on the shape of a pulsed function. Simultaneously with the transmitted pulse, a secondary magnetic field must be measured. The abrupt interruption of a stationary current flowing in a loop (Tx transmitter) disposed on the earth's surface induces secondary currents involving targets conductors (eddy currents) (Figure 3) (Morais & Menezes, 2005).

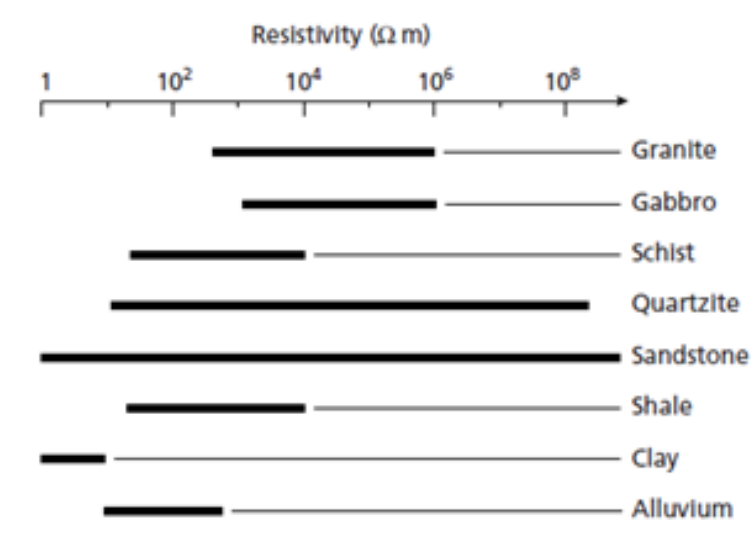


Figure 1 - Resistivity of some rocks and materials (Kearey et al., 2002).

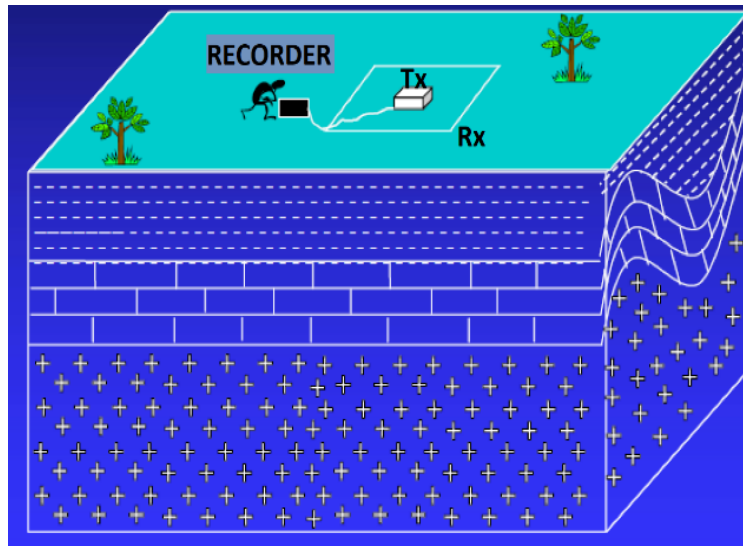


Figure 2 - Installation of equipment in a transient electromagnetic survey (Santos, 2006).

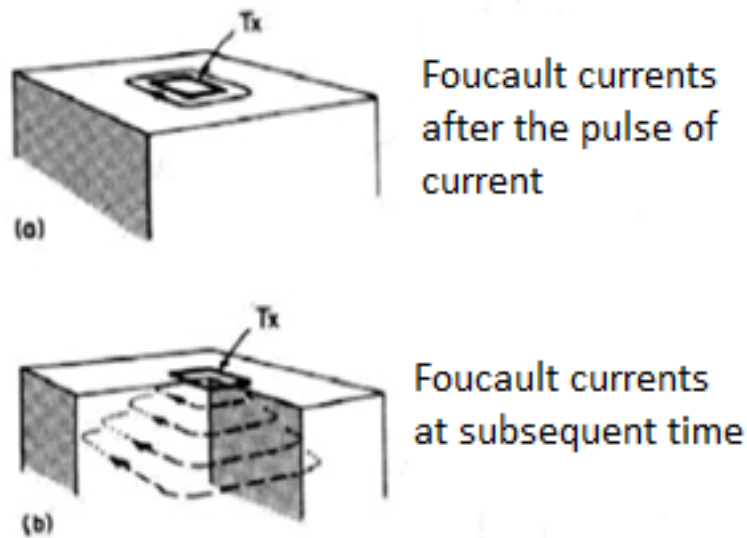


Figure 3 - Foucault current dissemination "eddy currents" (Morais & Menezes, 2005).

In a two-layer stratified model, at the beginning of the process called "Early Times", eddy currents are concentrated near the surface of the ground and the induced voltage is nearly constant. At this point, the voltage is proportional to the most superficial resistivity. With the diffusion of the eddy currents over time "Late Times", the voltage becomes proportional to $t^{-5/2}$ and $\rho^{-3/2}$, where t is the time and ρ is the resistivity of the deeper layers. This is illustrated by Figure 4, which shows the induced voltage for a coil of radius $a = 100$ m above a region of two layers, with the resistivity of the first layer constant and the resistivity of the second layer variable.

The apparent resistivity can be calculated with the voltage that would be measured above a resistivity homogeneous half-space ρ_1 :

$$\frac{\rho_a}{\rho_1} = \left| \frac{V_{un}(\rho_1, t)}{V_{obs}(t)} \right|^\lambda, \quad (2)$$

where ρ_a is the apparent resistivity, λ is a real number, V_{obs} is the observed voltage at time t and V_{un} is the voltage that would be observed in the half space ρ_1 at time t . Assuming a Late Stage for the field making $\lambda = 2/3$ in Eq. (2) (Kauffman & Keller, 1983), we obtain:

$$\rho_a = \frac{\mu}{4\pi t} \left| \frac{2\pi\mu r^2 M_r I}{5tV} \right|^{\frac{2}{3}}, \quad (3)$$

where μ is the magnetic permeability, r is the radius of the transmitter, M_r is the moment of the receiving coil, I is the transmission current, t is the time flowed after the attenuation of Eddy

currents and V is the voltage induced in the receiver coil.

According to Santos & Flexor (2008), in the acquisition of the transient electromagnetic method data, the most commonly used settings are described in Figure 5.

The coil dimensions, usually squares, ranging

from 1 x 1 m for shallow investigations to 2 x 2 km to a large depth investigation. By increasing the area of the transmitter loop, there is an improvement of the signal at the receiver, and then it is possible to investigate deeper structures. The current transmission occurs with positive and negative pulses (Figure 6).

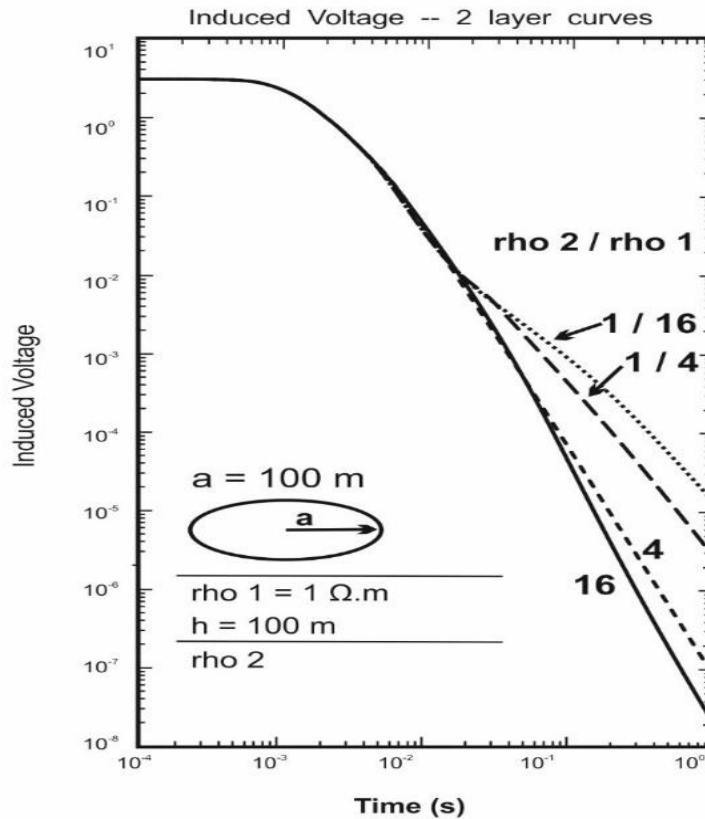


Figure 4 - Induced voltage as a function of time for a two-layer model.

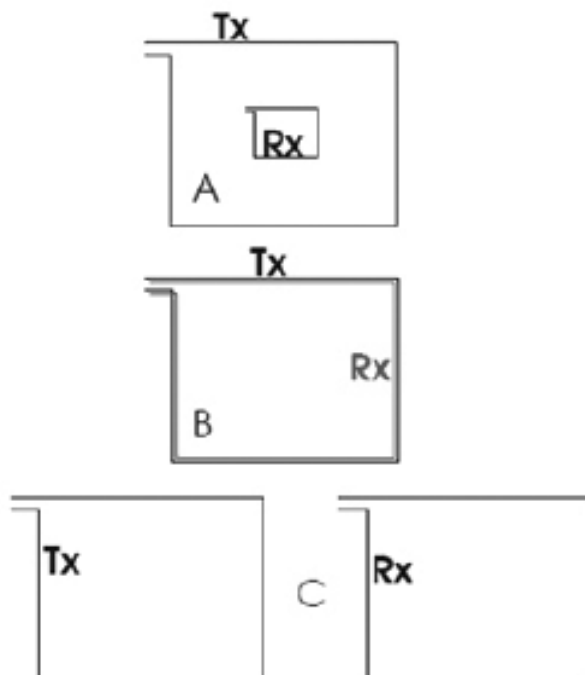


Figure 5 - Configuration of coils in the TEM method: “A” receiver coil located in the central part of the arrangement (In-Loop); “B” coincident coil or single coils; “C” coils placed laterally (Santos & Flexor, 2008).

During the pulses, a period in which no electric current is received occurs, so the signal is measured.

The pulse is transmitted several times in the measurements and then the attenuation time estimation is made through average results produced through a "stack" of measures (Santos, 2006).

With these considerations, the apparent

resistivity ρ_a can be calculated asymptotically through the formula:

$$\rho_a = 6.32 \times 10^{-12} \times A^2 \times b^4 \times \left(\frac{V}{I}\right)^{-2} \times t^{-5}, \quad (4)$$

Where ρ_a is the apparent resistivity, A is the loop effective area, b is the coil side length, (V/I) is the transient response and t is the operating time (Kaufmann & Keller, 1983).

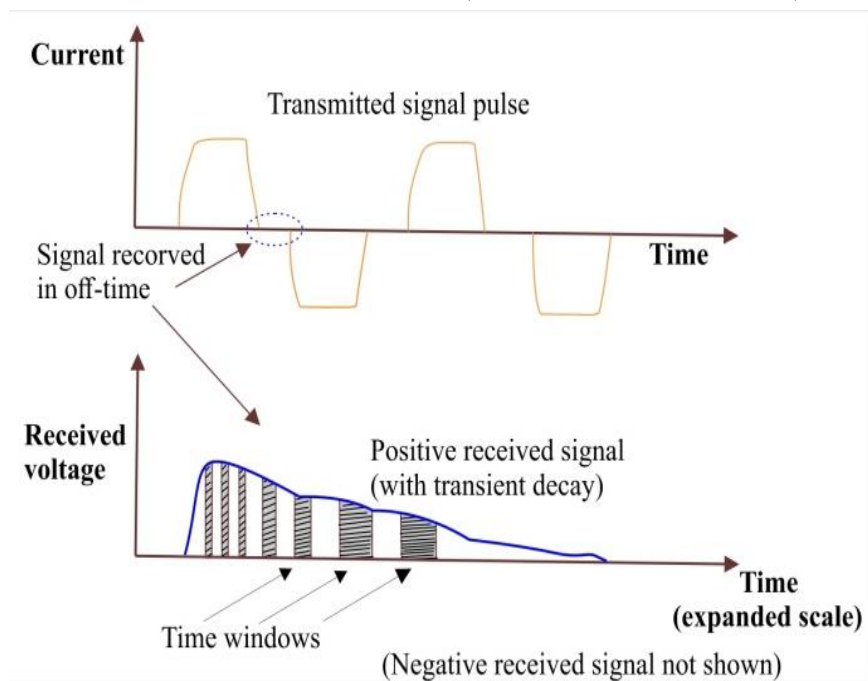


Figure 6 - Time evolution of the wave form in the transmitter and the voltage at the receiver. Redrawn after Santos (2006).

DESCRIPTION OF THE RESENDE BASIN

Location

The Resende Basin is located in the extreme southwest of Rio de Janeiro State between the Mantiqueira Sierra and the Bocaina Sierra. It is a segment covering Porto Real, Quatis, Barra Mansa (Florianópolis district), Resende and Itatiaia counties. The dimensions of the basin are 47 km long, 4.5 km average wide and 7.3 km at its widest portion in the west of Resende and 1.2 km minimum width in the west of Itatiaia (Santos & Flexor, 2008). It is located between the 22° 22' - 22° 30' S latitude and 44° 12' - 44° 30' W longitude (Figure 7).

The Basin is located between the Bocaina and Itatiaia national parks in a valley limited by Mar Serra and Mantiqueira Sierra. The region is on the Rio de Janeiro - São Paulo road axis, which are the major urban and industrial centers of Brazil. The geology of the Resende Basin is formed by alluvial - colluvial Cenozoic successions, overlaying the Precambrian metamorphic rocks and the magmatic intrusive

rocks of Mesozoic age to tertiary (Castro et al., 2000). The main sediments are sandstones, conglomerates and pelites. On the other hand, the crystalline basement consists mainly gneisses, migmatites, granitoids and quartzites (Bettini, 2004).

Resende Basin Topography

The Resende Basin is located in the morphostructural domain of the Rio Paraíba do Sul valley. The region is the lowest in the area along the Paraíba do Sul river. It covers alluvial plains and rounded by tabular hills with slightly flattened tops (Figure 8) (CASTRO et al., 2000).

The topographic map (Figure 9) locates the Resende Basin in a region of low altitude in relation to its vicinity. It is clear the basin location in a valley between the Mantiqueira Sierra and Bocaina Sierra. The alkaline massifs of Itatiaia and Morro Redondo in the northwest and southeast, respectively, are also well located. The altitude ranges from 400 m to around 2,100 m in the highest region.

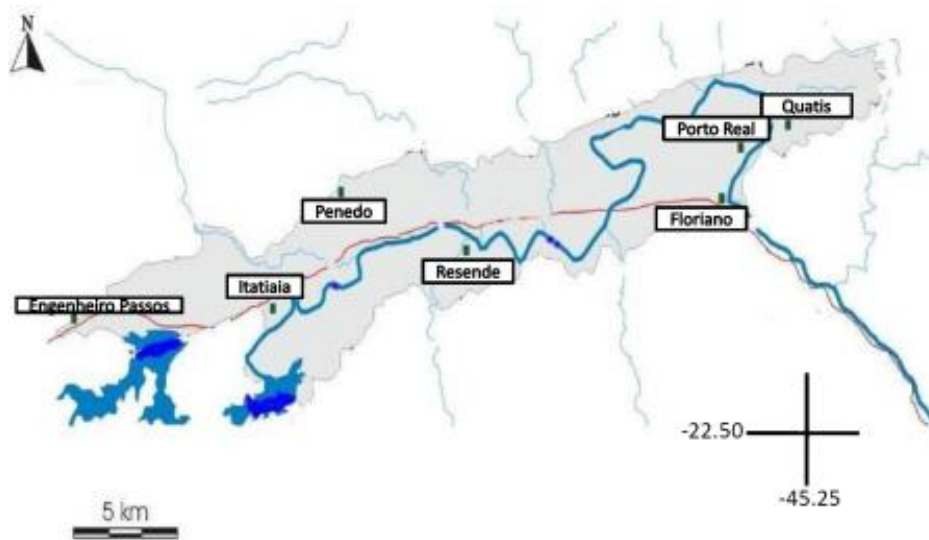


Figure 7 - Location of the Resende Basin (Bettini, 2004).

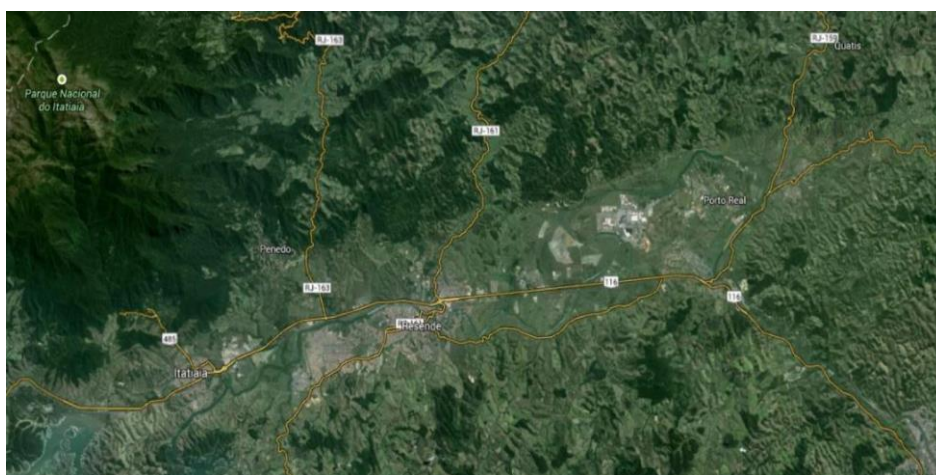


Figure 8 - Satellite view of the Resende Basin (Landsat, 2014).

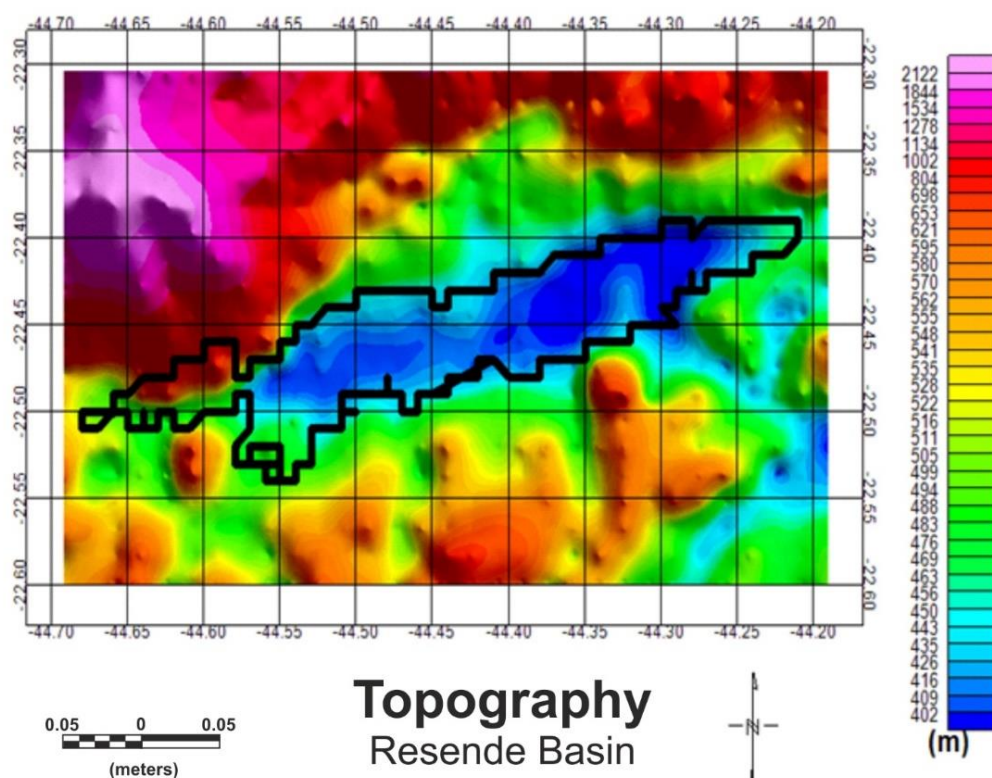


Figure 9 - Topographic map of the Resende Basin obtained from V16.1 Topex model.

Resende Basin Geology

Basically, the Resende Basin geology is formed by alluvial - colluvial cenozoic sequences, superimposed on Precambrian metamorphic rocks and intrusive magmatic rocks from Mesozoic to Tertiary age (CASTRO et al., 2000). Bettini (2004) summarized the Resende Basin geology through Figure 10.

Available Models

Previous research in Resende Basin provided important maps for the basin study. These maps are used for the consistency evaluation in the obtained results from this study.

Electrical Resistivity Model

Santos (2006) used the Transient Electromagnetic Method (TEM) to build a geoelectric image of the Resende Basin. The geoelectrical imaging showed the existence of three main areas: a central structural high flanked by two large depocenters, one at east and another on the west of the basin (Figure 11).

Gravimetric Modeling Of The Resende Basin

The gravimetric method is based on the Earth's gravity field measurements and their intensity variations caused by density changes in crustal rocks. Thus, the structural high (shallower regions) of a sedimentary basin increases the intensity of gravity in its vicinity. On the other hand, depocenters (deeper sediment regions) reduce the gravity strength.

A ground gravity survey was executed in the Resende Basin in 170 stations spaced almost evenly with an area of around 2 km spacing (Bettini, 2004). From these collected data, Escobar & Dias (1999) obtained a residual Bouguer anomaly map that formed the basis of the basin gravity modeling.

Then, as a result of the inversion which was linked to well data, it was obtained the model presented in Figure 12, in which, the observed curves are indicative of the Resende sedimentary basin thickness.

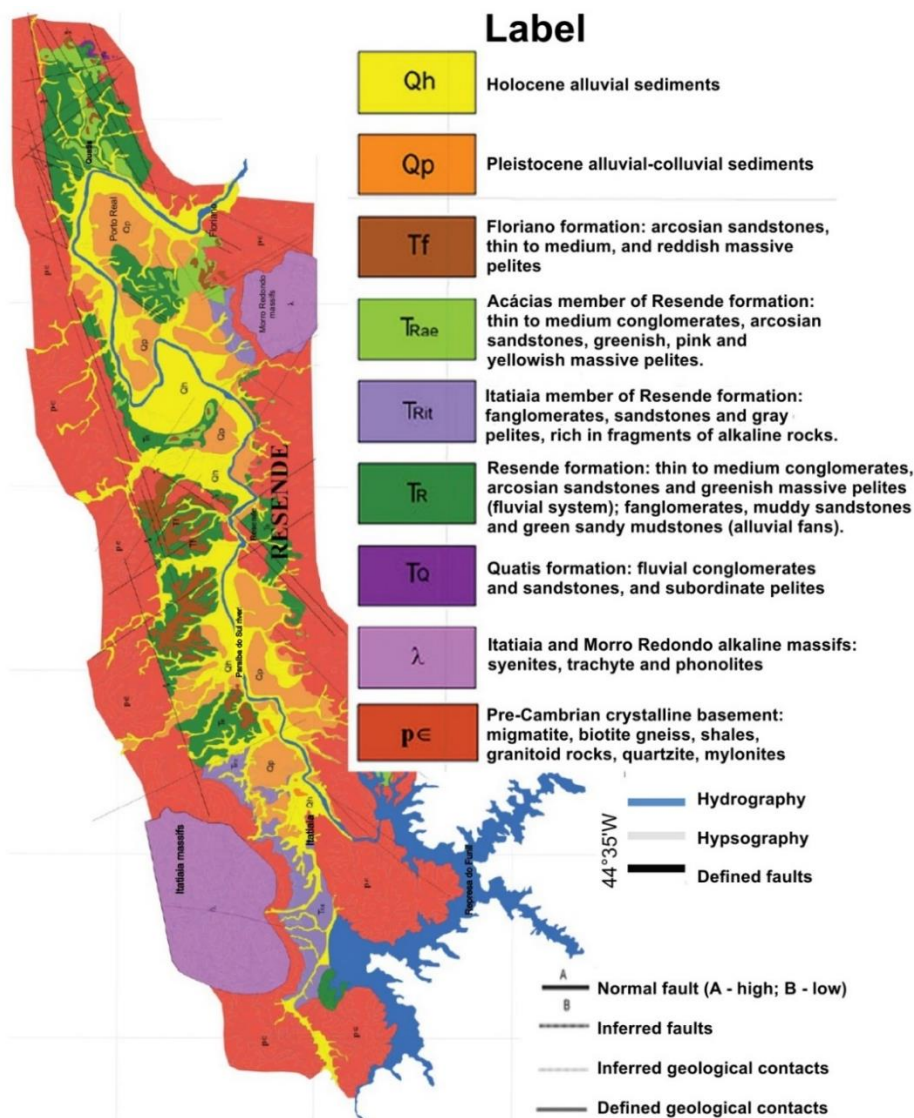


Figure 10. Geological map of the Resende Basin (Bettini, 2004).

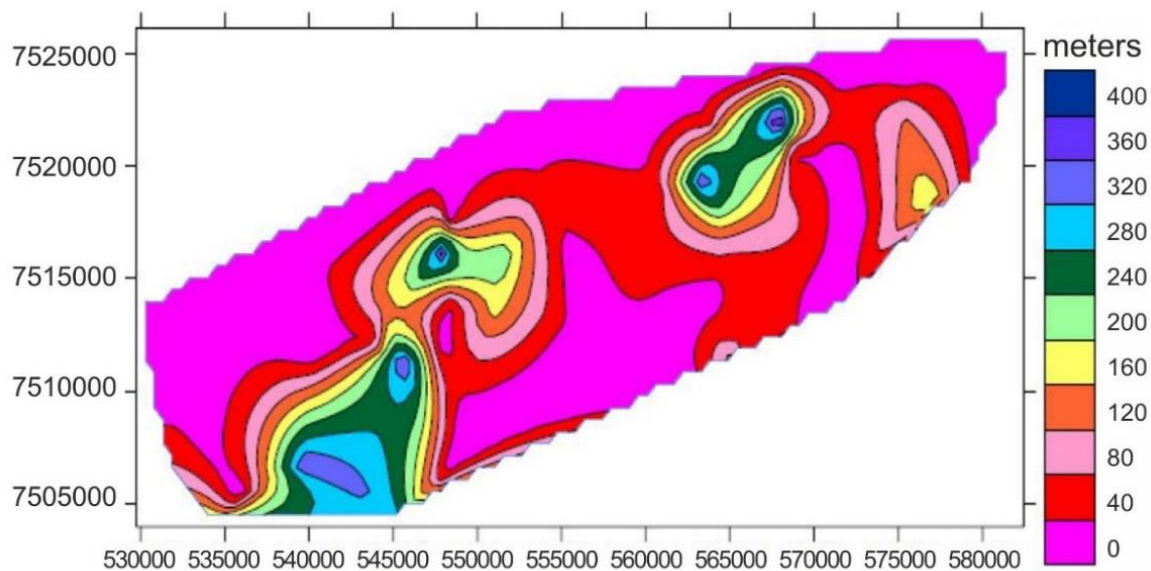


Figure 11 - Basement geoelectric image of the Resende Basin (Santos, 2006).

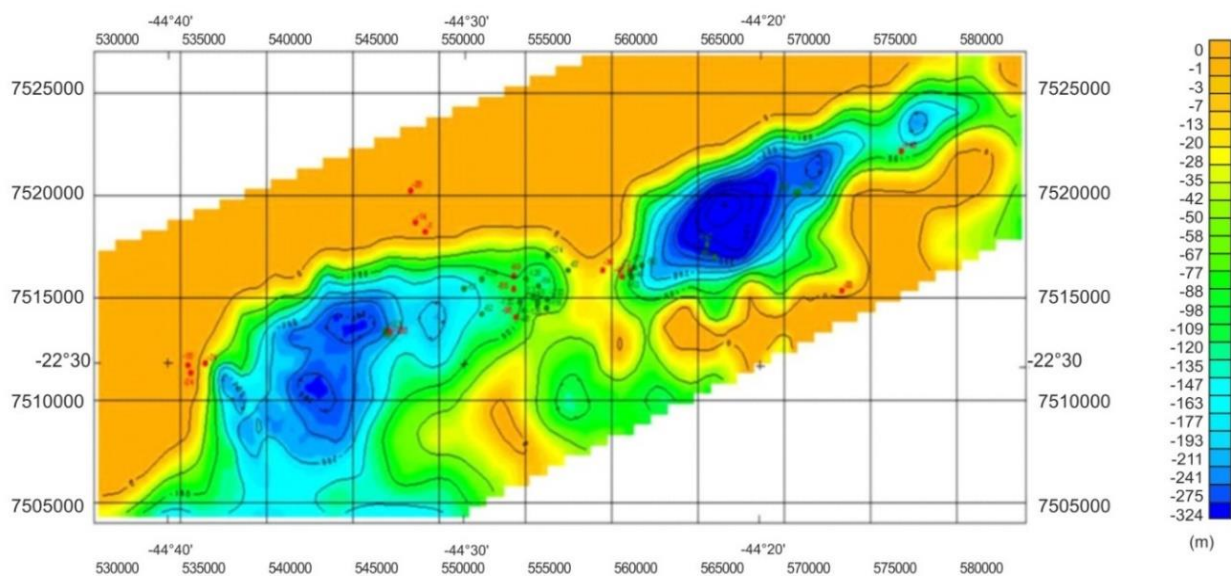


Figure 12 - Gravimetric modeling of the Resende Basin (Escobar & Dias, 1999).

PROCESS AND RESULTS

A group of 88 electromagnetic transient stations of the Resende Basin were used in this work (Figure 13). In the data acquisition, the In-Loop and Single Loop settings (Figure 5) were used in the SIROTEM MK3 equipment (Figure 14). In the In-Loop setting, only 77 stations were effectively used. In the other 11 stations, the signal was very weak and had poor quality, preventing the processing.

In the Single Loop setting, only 56 stations were actually used. In this case, some stations were not performed in this setting and in others the signal was very poor, disabling the processing, then totaling 32 unused stations.

The acquired data were processed through the 2.4.05 version of the Winglink program. The data consisted of the temporal voltage curve

perceived at the receiver.

A link to depth was used in processing, but the resistivity was left free to vary along the iterations.

The program, through a set of 10 iterations, estimated a 4-layer model of the apparent resistivity. We look for the depth where the apparent resistivity exceeded $300 \Omega.m$. This point was used as a cutoff for the geoelectrical imaging confection (Figure 15). The processing of the maps was performed with the Oasis Montaj Geosoft software. The maps were obtained by data interpolation with the Minimum Curvature technique, using 500 meter cells. The processing allowed to obtain two map types: isovalue map and pseudo-3D map for Single Loop and In-Loop settings.

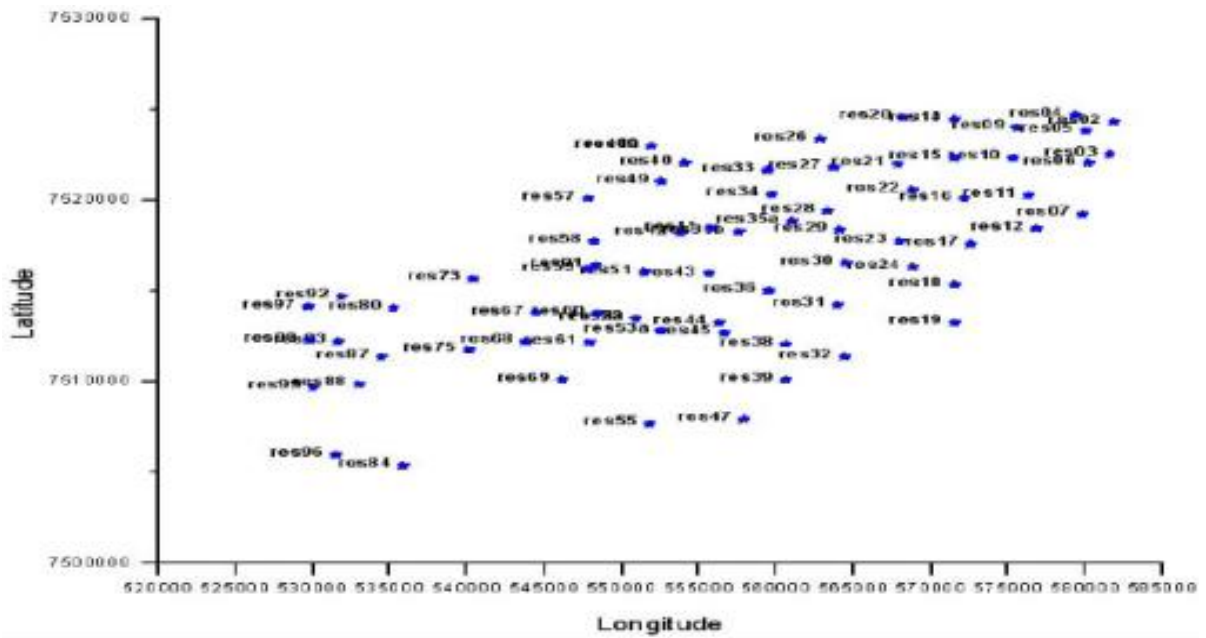


Figure 13 - Station positions in the Resende Basin.



Figure 14 - SIROTEM MK3 equipment of Geoinstruments Ply Ltd.

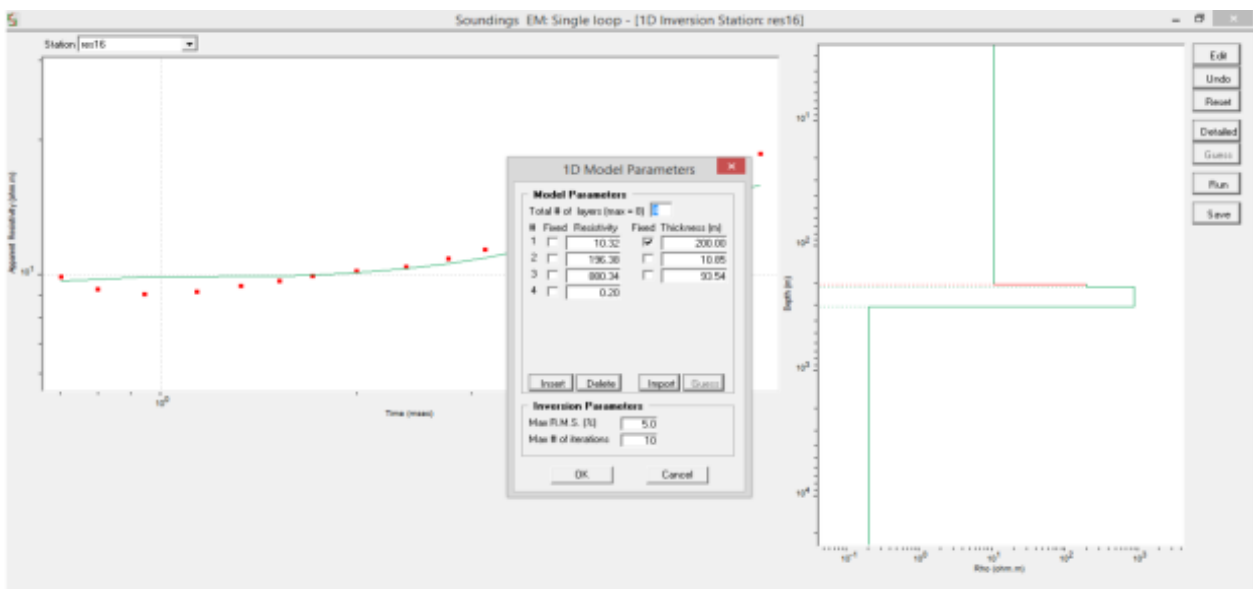


Figure 15 - Construction of the resistivity model.

In possession of these acquired depths, the isovalue geoelectrical map of the Resende Basin in the In-Loop setting with $\rho < 300 \Omega.m$ was created (Figure 16).

The geoelectrical map obtained in the configuration In-Loop shows that the basin was very well characterized in a lower altitude region between the Mantiqueira Sierra and the Mar Sierra. The In-Loop geoelectrical map was compared with the maps of previous studies: the gravity inversion map (Figure 12) obtained by Escobar and Dias (Escobar & Dias, 1999) and the geoelectrical model obtained by Santos (2006) (Figure 11).

The comparison of the maps of Figures 11, 12

and 16 led to a compatible result. It showing a basin with just over 300 meters deep in its depocenters. When compared to the geological map (Figure 10), the Figure 16 shows that the deeper sediments are associated with alluvial sediments, conglomerates, sandstones and pelites from the Resende Formation present in abundance in the east and west borders of the basin (Bettini, 2004).

A pseudo-3D map (Figure 17) was obtained with In-Loop setting. It illuminates efficiently the depocenters (deepest parts) of the Resende Basin. A less deep and central conductive region is also noted. Furthermore, the northern and southern limits of the basin can also be well identified.

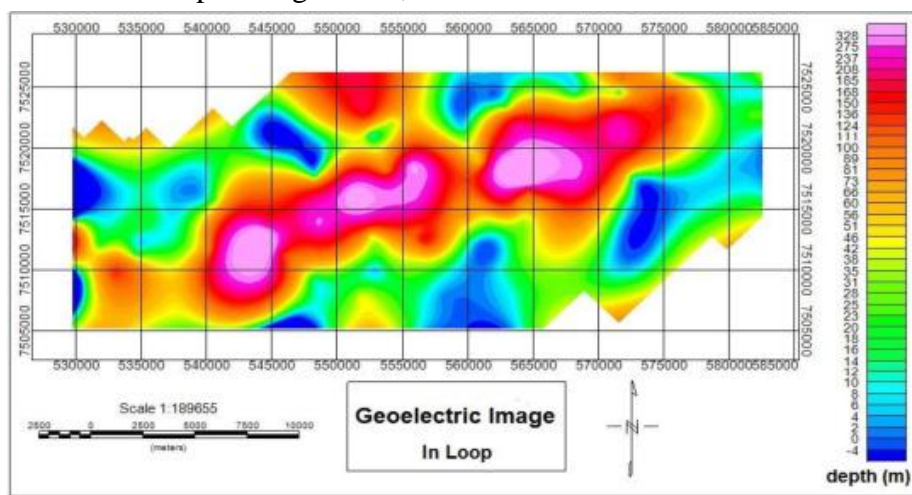


Figure 16 - Geoelectric Image ($\rho < 300 \Omega.m$) in the In-Loop setting.

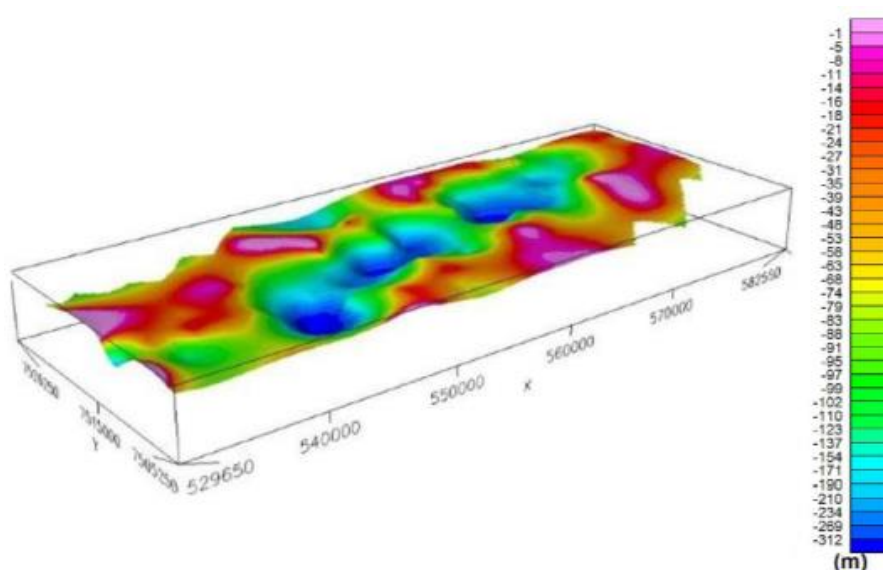


Figure 17 - Pseudo-3D map ($\rho < 300 \Omega.m$) in the In-Loop setting.

The processing of the 56 Single Loop stations allowed the construction of the isovalue depth map where $\rho < 300 \Omega.m$ (Figure 18). Even with only 56 useful acquisitions of the Single Loop configuration, the major topographic and geological features of the basin also appear on the

map of Figure 18. In addition, the map showed higher accordance with the gravimetric modeling map (Figure 12) obtained by Escobar and Dias (Escobar & Dias, 1999) and the geoelectrical model (Figure 11) obtained by Santos (Santos, 2006), mainly in the eastern part of the basin.

It was also made a Pseudo-3D map of the geoelectrical imaging in the Single Loop setting (Figure 19). The deeper and more conductive parts of the basin can be seen on both maps.

The geoelectric maps obtained (Figures 16, 17, 18 and 19) allow us to estimate the lateral limits and depth of the Resende Basin. Additionally, they reveal the most electrically conductive parts of the basin.

The geoelectrical mapping of the Resende Basin was able to separate the sediment (more conductive) and the crystalline (less conductive) regions.

Therefore, it can be useful for differentiation

in the drilling of new wells in sedimentary, crystalline and mixed aquifers.

Furthermore, the obtained resistivity contrasts can be useful when combined with other studies for mineral prospecting.

The transient electromagnetic method was well implemented in the Resende Basin, because it is a shallow sedimentary basin. However, some sediment regions can be much deeper than estimated. Whereas when the geological material is very conductive, the eddy currents drain fast, preventing further measures. Therefore, it is recommended to further research the using of magnetotelluric surveys that can reach greater depths.

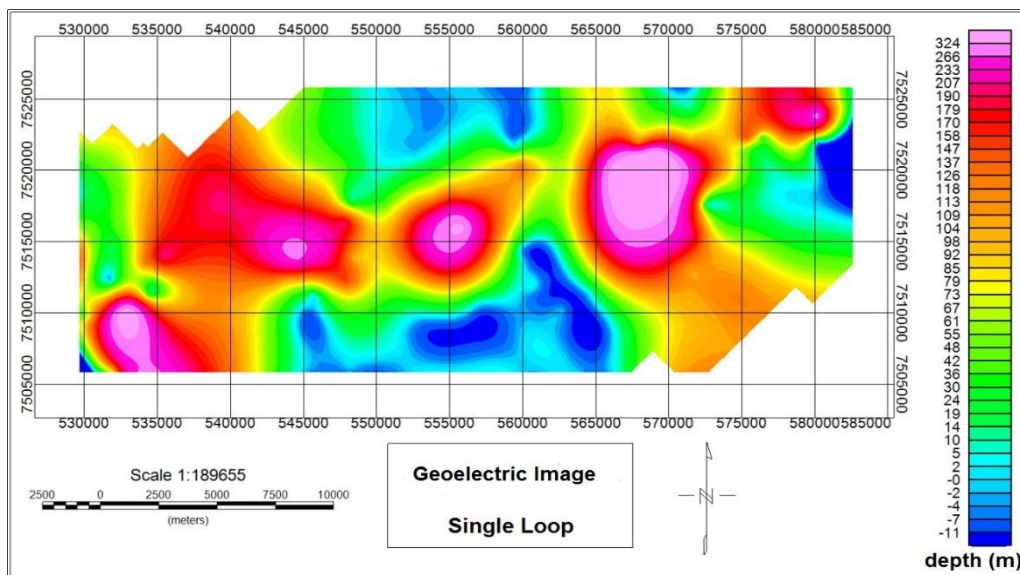


Figure 18 - Geoelectric Image ($\rho < 300 \Omega.m$) in the Single Loop setting.

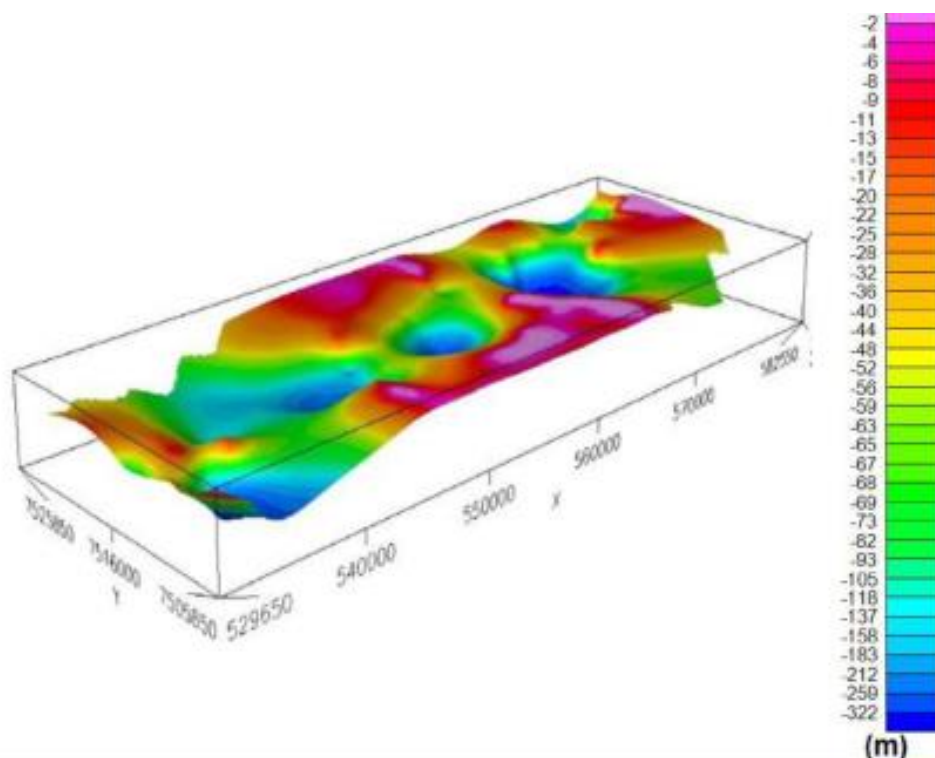


Figure 19 - Pseudo-3D map ($\rho < 300 \Omega.m$) in the Single Loop setting.

CONCLUSIONS

Two electrical resistivity models of the Resende sedimentary basin were created through 88 transient electromagnetic surveys and 39 well data. These models may be considered an update of the previous models, as well data were directly incorporated in the near resistivity stations. Soon, they are more realistic. Through the generated maps, we can visualize the borders and the depths of sediment and more conductive materials ($\rho < 300 \Omega.m$) which constitute the basin. The basin was well located in a valley between the Mar Sierra and Mantiqueira Sierra. Thus, there was

good agreement with previous research (gravimetric and electrical resistivity).

The resistivity maps from acquiring data with the In-Loop and Single Loop settings generated very similar maps that show the main basin features. The biggest difference between them occurs in the eastern region of the Single Loop map that appeared to be deeper than on the In-Loop map. Even with fewer stations, the resistivity map from Single Loop setting appeared to be more consistent with the gravity maps obtained in previous studies.

REFERENCES

- BETTINI, C. **Modelagem estratigráfica de reservatório terrígeno: Aplicação à avaliação do potencial hídrico da Bacia de Resende (RJ)**. Projeto Modesthi. Relatório Final, 278 p., 2004.
- CASTRO, F.G.; JUNIOR, G.C.S.; PIZANI, T.C.; SILVA, D.B. Caracterização Hidrogeológica e Hidrogeoquímica Preliminar da Bacia Sedimentar de Resende- RJ. In: JOINT WORLD CONGRESS ON GROUNDWATER, 1st, 2000.
- DELLEUR, J.W. **The Handbook of Groundwater Engineering**. Second Edition, CRC Press. 1320 p. 2006.
- ESCOBAR, I.P. & DIAS, F.S.S. **Mapa Bouguer Residual da Bacia de Resende**. Comunicação pessoal. 1999.
- KAUFMANN, A.A. & KELLER, G.V. Frequency and Transient soundings. In: KAUFMANN, A.A. & KELLER, G.V., **Series in Methods in Geochemistry and Geophysics**, Elsevier, 16: 685p. 1983.
- KEAREY, P.; BROOKS, M.; HILL, I. **An Introduction to Geophysical Exploration**. Berlin, Black Science Ltda., 3ª ed, 2002.
- MORAIS, E.R. & MENEZES, P.T.L. Estratigrafia Geométrica da Seção Carbonática da Bacia de Sergipe-Alagoas, Região do Campo de Riachuelo, Sergipe. **Revista de Geologia**, v. 18, n. 2, p.175-185, 2005.
- PENG, S. & ZHANG, J. **Engineering Geology for Underground Rocks**. Springer, 320 p., 2007.
- SANTOS, F.M. **Aplicação de Métodos Geofísicos no Estudo da Contaminação de Águas Subterrâneas no Lixão de Cuiabá-MT**. Cuiabá, 2005. 101 p. Dissertação (Mestrado em Física e Meio Ambiente), Instituto de Ciências Exatas e da Terra - Universidade Federal de Mato Grosso.
- SANTOS, H.S. & FLEXOR, J.M. O Método Transiente Eletromagnético (TEM) Aplicado ao imageamento geoeletrico da Bacia de Resende (RJ, Brasil). **Brazilian Journal of Geophysics**, v. 26, n.4, p. 543-553, 2008.
- SANTOS, H.S. **O Método Transiente Eletromagnético. Aplicação ao Estudo da Estrutura Geométrica da Bacia de Resende (RJ, Brasil)**. Rio de Janeiro, 2006. 71 p. Dissertação (Mestrado em Geofísica) - Observatório Nacional.
- SCHMUCKER, U. & WEIDELT P. **Electromagnetic Induction in the Earth**. Lecture notes (not published), University of Aarhus, Germany, 1975.
- SORENSEN, K.I.; AUKEN, E.; THOMSEN, P. TDEM in Groundwater Mapping – a Continuous Approach. In: SYMPOSIUM ON THE APPLICATION OF GEOPHYSICS TO ENGINEERING AND ENVIRONMENTAL PROBLEMS (SAGEEP), 13, 2000. Arlington, VA: **Extended abstract**, 2000, p. 485-492.

*Submetido em 24 de julho de 2018
Aceito em 11 de março de 2020*